Journal of Thermal Analysis and Calorimetry, Vol. 88 (2007) 1, 139–144

PARTIAL THERMAL REDUCTION OF AMMONIUM PARATUNGSTATE TETRAHYDRATE
Evolved gas analysis (TG/DTA-MS) and solid state studies (XRD, FTIR)

I. M. Szilágyi[1*], *J. Madarász*[1], *F. Hange*[2] *and G. Pokol*[1]

[1]Institute of General and Analytical Chemistry, Budapest University of Technology and Economics, 1111 Budapest Szt. Gellért tér 4, Hungary
[2]GE Hungary ZRt., GE Consumer & Industrial - Lighting, 1340 Budapest, Váci út 77, Hungary

Thermal decomposition of ammonium paratungstate tetrahydrate, $(NH_4)_{10}[H_2W_{12}O_{42}]\cdot 4H_2O$ has been followed by simultaneous TG/DTA and online evolved gas analysis (TG/DTA-MS) in flowing 10% H_2/Ar directly up to 900°C. Solid intermediate products have been structurally evaluated by FTIR spectroscopy and powder X-ray diffraction (XRD). A previously unexplained exothermic heat effect has been detected at 700–750°C. On the basis of TG/DTA as well as H_2O and NH_3 evolution curves and XRD patterns, it has been assigned to the formation and crystallization heat of γ-tungsten-oxide ($WO_{2.72}$/$W_{18}O_{49}$) from β-tungsten-oxide ($WO_{2.9}$/$W_{20}O_{58}$) and residual ammonium tungsten bronze.

Keywords: *FTIR spectroscopy, mass spectrometry, simultaneous TG/DTA, tungsten, X-ray diffraction*

Introduction

Ammonium paratungstate tetrahydrate (APT), $(NH_4)_{10}[H_2W_{12}O_{42}]\cdot 4H_2O$ is a starting material of tungsten lamp filament production [1–3]. Partial reduction of the title compound between 400 and 600°C produces an intermediate product (called 'tungsten blue oxide', TBO), which is a possible mixture of different phases (X-ray amorphous phase, WO_3, $WO_{2.9}$/$W_{20}O_{58}$, $WO_{2.72}$/$W_{18}O_{49}$, WO_2, tungsten bronzes [1, 2, 4–9]). 'Tungsten blue oxide' is doped with K, Al and Si. This provides after a complete reduction in hydrogen an appropriate mechanical stability (a so-called 'non-sag' feature) to tungsten wires even at high operating temperatures in lamps [1–3].

In addition, the reduction of APT or 'tungsten blue oxide' to tungsten metal is a vital step in the production of tungsten carbide (WC). Tungsten carbide is the basic and most widely used hard component of cemented carbides or hard metals, which are used in the production of cutting, mining, machining and forming devices [1, 9–12]. Furthermore WC and also W_2C can act as catalysts in a great variety of oxidation/reduction reactions like hydrogenolysis, alcane reforming, etc. [1, 13, 14].

A better understanding of the thermal reduction of APT is necessary for a better production of tungsten metal for the needs of tungsten based hard metals and catalysts, and is also very useful as a comparison tool when studying the reduction of undoped and doped 'tungsten blue oxide'.

Earlier studies focused mainly on the reduction of APT up to 400–600°C, because researchers were interested mostly in the formation of 'tungsten blue oxide' ([7, 8] and references therein). In our previous work we studied also the thermal decomposition of APT up to 400–600°C [15–17].

About the reduction of APT over 400–600°C mostly TG curves were published [18–23]. According to these studies and ex situ [22] as well as in situ [23, 24] XRD analyses, from the tungsten bronzes formed from APT around 300–500°C, reduced tungsten oxides ($WO_{2.9}$/$W_{20}O_{58}$, $WO_{2.72}$/$W_{18}O_{49}$, WO_2) and finally β- and α-tungsten are produced. Their formation is highly influenced by experimental conditions (reducing atmosphere, sample amount, layer thickness, particle size, etc.) [1, 2, 7]. Over 400–600°C, the few published DTA results showed one or two endothermic heat effects [5, 19, 21, 22] and an unexplained exothermic DTA peak [5]. To the best of our knowledge only Gerey performed evolved gas analytical (EGA) measurements above 400–600°C ([25] and the observed evolution curves cited as figures in [24, 26]), which indicated further release of water, ammonia and even to a small extent that of nitrogen in stepwise reactions.

The few number of EGA and DTA results on the reduction of APT at elevated temperatures encouraged us to reinvestigate the reduction of APT. This idea was

* Author for correspondence: imre.szilagyi@mail.bme.hu

1388–6150/$20.00

Akadémiai Kiadó, Budapest, Hungary
Springer, Dordrecht, The Netherlands

further supported by the existing interest of researchers in the thermal properties of tungsten oxides [9, 15–17, 22, 23, 27, 28], and also by a recent TG-MS study on un-doped and doped WO_3, which demonstrated the usefulness of evolved gas analysis on the reduction of tungsten oxides above 400–600°C [27].

Here as an attempt to get a deeper insight into the partial reduction of APT, particularly at elevated temperatures, we carried out on-line evolved gas analysis (TG/DTA-MS) and solid-state studies (FTIR and XRD) in flowing 10% H_2/Ar directly up to 900°C.

Experimental

Ammonium paratungstate tetrahydrate (H. C. Starck GmbH), $(NH_4)_{10}[H_2W_{12}O_{42}]\cdot 4H_2O$ (ICDD 40-1470) was subjected to thermal analysis as received. XRD and FTIR (KBr) measurements did not show any impurities in the APT sample.

Open platinum crucible, a heating rate of 10°C min^{-1}, sample size of 149.7 mg and flowing 10% H_2/Ar (130 mL min^{-1}) were used for purging the thermoanalytical furnace during the evolved gas analytical measurements.

The TG/DTA-MS apparatus consisted of an STD 2960 simultaneous DTA/TGA (TA Instruments Inc.) thermal analyzer and a Thermostar GSD 200 (Balzers Instruments) quadrupole mass spectrometer. On-line coupling between the two parts was provided through a heated (T=200°C) 1 m 100% methyl deactivated fused silica capillary tube with inner diameter of 0.15 mm. A mass range between m/z=1–64 was monitored through 64 channels in multiple ion detection mode (MID) with a measuring time of 0.5 s/channel.

The components of released gaseous mixtures were monitored and identified on basis of their MS reference gas spectra [29].

Intermediate solid samples were obtained from 170, 240, 365, 450°C heated at 5°C min^{-1} and from 570, 670, 750°C heated at 10°C min^{-1} in a Setaram TG/DTA 92 apparatus in 10% H_2/Ar (75 mL min^{-1}) in open Pt crucible (m_0=80–100 mg), as well as from 900°C heated at 10°C min^{-1} in an STD 2960 simultaneous DTA/TGA (TA Instruments Inc.) apparatus in 10% H_2/Ar (130 mL min^{-1}) in open Pt crucible (m_0=149.7 mg). Heating rates and temperatures were determined so that these intermediate samples represent the solid state structure after each main decomposition step.

FTIR spectra of intermediates were measured between 400–4000 cm^{-1} by an Excalibur Series FTS 3000 (Biorad) FTIR spectrophotometer in KBr pellets.

Powder X-ray diffraction (XRD) patterns of intermediates were recorded on a Philips MPD 1880 X-ray diffractometer between 2θ=5–65° at 0.02°/1 s with $CuK_{\alpha\ 1,2}$ radiation.

Results and discussion

The TG, DTG and DTA curves of the reduction of APT are presented in Fig. 1. Eight decomposition steps were observed up to 900°C, which are marked on the DTG curve.

On the basis of MS signals (Table 1), evolution of water, ammonia and to a small degree that of nitrogen were detected (Fig. 2).

FTIR spectra and X-ray diffractograms of intermediates are shown in Figs 3 and 4, respectively. When in the intermediates more crystalline phases were present (from 450°C), their main reflections were marked on the XRD patterns (Fig. 4).

Table 1 Ions of molecules detected by TG/DTA-MS during the thermal decomposition of APT in 10% H_2/Ar

m/z	Ion	Source molecule
14	N^+	NH_3, N_2
15	NH^+	NH_3
16	NH_2^+	NH_3
	O^+	H_2O
17	NH_3^+	NH_3
	OH^+	H_2O
18	H_2O^+	H_2O
19	HDO^+	HDO
28	N_2^+	N_2

Formation of tungsten bronzes

Here, based on our previous studies [16, 17], the main features of the partial reduction of APT up to 450°C are discussed with some additional comments.

In the first decomposition step (50–170°C) in an endothermic reaction (Fig. 1) with the evolution of adsorbed and chemisorbed water (Fig. 2) APT decomposed partially (the 1.81% mass loss is equivalent to ~2.5H_2O molecules). In the infrared spectrum the deformation bands at 1622 and 1680 cm^{-1} suggests water molecules bounded differently (Fig. 3). During the evolution of water the band at 1680 cm^{-1} disappeared completely at 170°C, and was accompanied by a decrease in the intensity of the broad band above 3000 cm^{-1} belonging to N–H, O–H vibrations (Fig. 3). The structure at 170°C was between that of APT (ICDD 40-1470) and dehydrated APT, $(NH_4)_{10}W_{12}O_{41}$ (ICDD 25-0045) (Fig. 4).

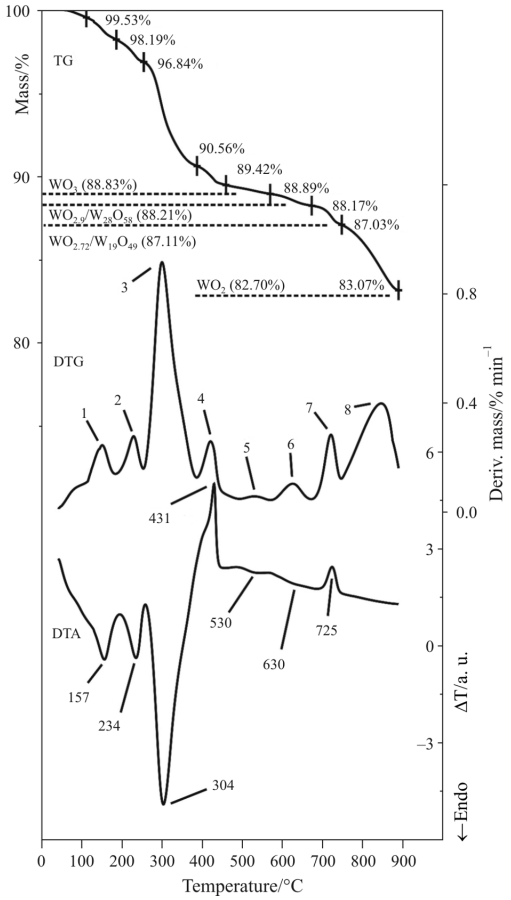

Fig. 1 Simultaneous TG/DTG/DTA curves of APT measured in 10% H_2/Ar (130 mL min^{-1}, 10°C min^{-1}, open Pt crucible, 149.7 mg). The dashed lines show the theoretical composition corresponding to the average mass level

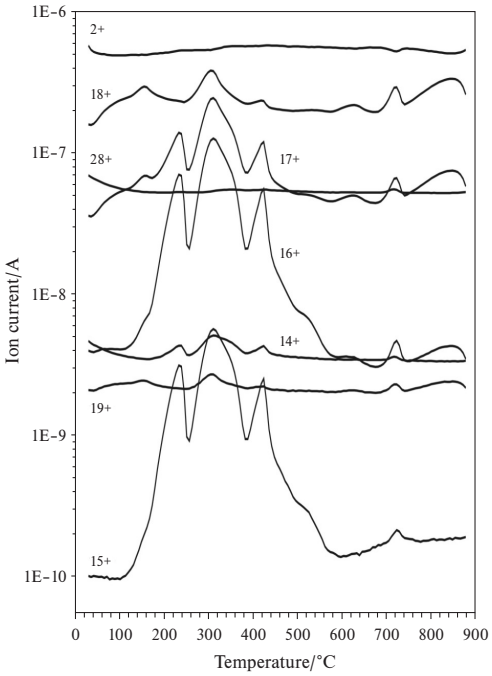

Fig. 2 Ion current curves of gaseous species evolved from APT measured by on-line coupled TG/DTA-MS system in 10% H_2/Ar (130 mL min^{-1}, 10°C min^{-1}, open Pt crucible, 149.7 mg)

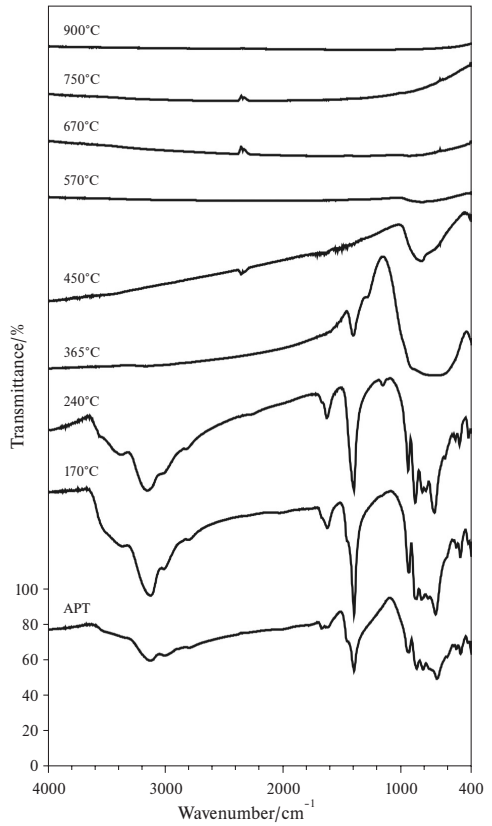

Fig. 3 FTIR spectra of intermediate solid products of APT decomposed in 10% H_2/Ar

Between 170–240°C in the second decomposition step in an endothermic reaction (Fig. 1) dry NH_3 (Fig. 2) was released (the 1.35% mass loss is equivalent to ~2NH_3 molecules) leaving a proton of NH_4^+ ion in the solid phase. The deformation bands at 1401 and 1462 cm^{-1} suggests differently bounded NH_4^+ ions (Fig. 3). The shoulder at 1462 cm^{-1} disappeared completely at 240°C, and the intensity of the broad band above 3000 cm^{-1} decreased further (Fig. 3). We could not confirm on the basis of the XRD pattern whether the solid sample at 240°C consisted of ammonium metatungstate, $(NH_4)_6[H_2W_{12}O_{40}]\cdot 2H_2O$ [7, 8] or a so-called APT II, $(NH_4)_8[H_2W_{13}O_{43}(OH)_2]\cdot H_2O$ phase [30] (Fig. 4). Note that to the best of our knowledge there is no ICDD card for either of these phases.

In the third decomposition step (240–365°C) in an endothermic reaction (Fig. 1) NH_3 and H_2O were released (Fig. 2). The deformation band of water at 1622 cm^{-1} disappeared completely, while that of NH_4^+ ion at 1401 cm^{-1} and the broad band above 3000 cm^{-1} reduced a great deal (Fig. 3). As a result of the collapse of the previous structure (linkage of WO_6 octahedra of separate paratungstate ions [17]) an

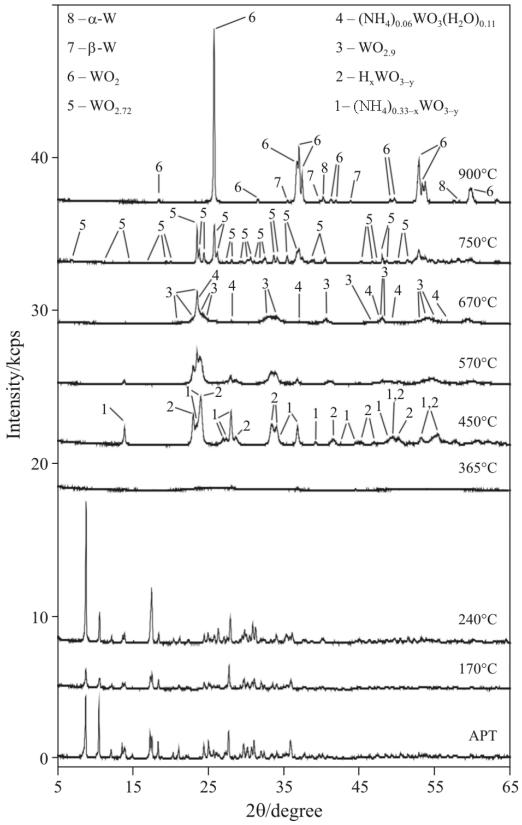

Fig. 4 XRD patterns of intermediate solid products of APT decomposed in 10% H_2/Ar. When in the intermediates more crystalline phases were present (from 450°C), their main reflections were marked on the XRD patterns

X-ray amorphous phase was formed (Fig. 4), which is also shown by the alteration of the region of W–O bonds below 1000 cm^{-1} (Fig. 3).

In the fourth decomposition step (365–450°C) NH_3 and H_2O were released (Fig. 2), the deformation band of NH_4^+ ion at 1401 cm^{-1} disappeared completely (Fig. 3). From the X-ray amorphous phase tetragonal hydrogen tungsten bronze (THTB), H_xWO_{3-y} (ICDD 23-1448) and hexagonal ammonium tungsten bronze (HATB), $(NH_4)_{0.33-x}WO_{3-y}$ (ICDD 42-0452) formed (Fig. 4). In our previous paper [16] we assigned the earlier unexplained exothermic heat effect at 400–450°C to the crystallization heat of these bronzes (Fig. 1). The microcrystallites of the bronzes might have already been present in the X-ray amorphous phase (in the fourth step only small changes occurred in the IR spectrum in the region below 1000 cm^{-1} as can be seen in Fig. 3), therefore the exothermic heat effect might have belonged mostly to the decrease in surface Gibbs energy due to the growth of crystallites of the formed tungsten bronzes.

Recently we discussed how the heating program influenced the formation of tetragonal hydrogen and hexagonal ammonium tungsten bronzes during the partial reduction of APT [17]. Based on semiquantitative XRD phase analysis described earlier [17], here the ratios of HATB and THTB were 34 and 66%, respectively, which clearly shows that the slow heating of APT is favourable for the formation of the tetragonal bronze.

In addition, based on the evolved gas analytical measurements, formation of these bronzes seems to be two overlapping processes. On the right side of the third DTG peak a shoulder can be seen, which suggests that there is an overlapping reaction between the third and the fourth decomposition steps (Fig. 1). This overlapping reaction is also detectable on the DTA curve between the third (304°C) and fourth (431°C) DTA peaks. While at the third decomposition step on the right side of ammonia evolution curves the shoulder belonging to the overlapping reaction is also observable, no shoulder can be seen on the right side of water evolution curves at the third step (Fig. 2). This means that at 320–380°C mostly ammonia was released. Therefore this overlapping reaction might belong to the formation of microcrystalline, i.e. X-ray amorphous tetragonal hydrogen tungsten bronze, since this process should be accompanied by the evolution of dry ammonia. Namely in this case a proton of NH_4^+ ion could remain in the solid phase and help the formation of THTB. Formation of microcrystalline hexagonal ammonium tungsten bronze could have already started before the formation of THTB, because Dickens *et al.* reported that HATB was present already from 285°C, when they annealed APT in reducing atmosphere in a furnace [31].

Formation of reduced tungsten oxides

In the fifth decomposition step (450–570°C) small amount of ammonia was released (Fig. 2) in a slightly endothermic reaction (Fig. 1). The amount of THTB and HATB was reduced and β-tungsten oxide, $WO_{2.9}/W_{20}O_{58}$ (ICDD 05-0386, 36-0102) was formed (Fig. 4). In the infrared spectrum the peak in the region below 1000 cm^{-1} reduced a great deal showing changes in W–O bonds (Fig. 3). From this stage the infrared spectra of intermediate samples was not informative enough, therefore they are not discussed further on.

In the sixth decomposition step (570–670°C) also small amount of water was released (Fig. 2) in a slightly endothermic reaction (Fig. 1). The main component of the sample at 670°C was $WO_{2.9}/W_{20}O_{58}$, which is not a well defined crystalline phase, according to Booth *et al.* [32]. This explains why the reflections of this sample were diffuse and not sharp enough. Because of the poor resolution of the reflections, the analysis of the minor components had larger uncertainty.

While THTB disappeared completely by 670°C, an ammonium tungsten bronze phase, $(NH_4)_{0.06}WO_3(H_2O)_{0.11}$ (ICDD 15-0217) with small ammonium ion content seemed to be still present (Fig. 4). In addition, traces of γ-tungsten oxide, $WO_{2.72}/W_{18}O_{49}$ (ICDD 05-0392) were supposed to be in this sample.

Neugebauer *et al.* [18] and later Mészáros *et al.* [24] reported the $(NH_4)_{0.06}WO_3(H_2O)_{0.11}$ phase to be tetragonal. Dickens and Wittingham ([33] and cited in [7]) disputes the existence of such a tetragonal phase, because the inscribed spheres of available cavities are too small for ammonium ions in the tetragonal tungsten bronze structure. Zou *et al.* (cited in [7]). reported the presence of three ammonium tungsten bronzes (ATB) during the reduction of APT: ATB' with high, ATB with normal, and ATB'' with low ammonium ion content and low oxygen index. They proposed that these ammonium tungsten bronzes had identical crystal lattices, i.e. hexagonal. The ammonium tungsten bronze detected by us at 670°C might have been the ATB'' phase mentioned by Zou *et al.*, but this question was left open, because the small amount of this compound in the intermediate sample and the poor resolution of the reflections did not allow proper structure elucidation.

In the seventh decomposition step (670–750°C) besides the evolution of water and ammonia, the release of nitrogen was also detected, and as a pronounced sign of the ongoing reduction a negative peak was observable on the hydrogen MS curve (Fig. 2). The observed nitrogen evolution corroborates with the results of Gerey [25], the main source of nitrogen could have been a reversed ammonia synthesis in the gas phase [34]. Nitrogen and thus ammonia evolution between 670–750°C indirectly prove that there was an ammonium tungsten bronze phase in the intermediate at 670°C and this confirms the correctness of the XRD analysis.

In the intermediate sample at 750°C, the main component was γ-tungsten oxide, $WO_{2.72}/W_{18}O_{49}$ (ICDD 05-0392, 36-0102). As a second phase δ-tungsten oxide, WO_2 (ICDD 32-1393) was observed, and only traces of $WO_{2.9}/W_{20}O_{58}$ could be detected (Fig. 4).

Between 700–750°C a previously (to the best of our knowledge) unexplained exothermic DTA peak was detected (Fig. 1), whose explanation we give below.

In the eight decomposition step (750–900°C) water was released as a reduction product of tungsten, which was accompanied again by a decrease in the hydrogen MS curve (Fig. 2). At this step no further heat effect was observed (Fig. 1). The intermediate at 900°C consisted of WO_2 with traces of β-tungsten, W_3O (ICDD 41-1230) and α-tungsten, W (ICDD 04-0806) (Fig. 4). The highly diluted reducing atmosphere might have been responsible for that tungsten metal started to form only at 900°C in our experiments, while in earlier studies performed in pure hydrogen tungsten started to form already at 550–600°C [1, 7, 8].

Discussion of the exothermic heat effect between 700–750°C

At first look, the exothermic heat effect between 700–750°C might be related to the appearance of either $WO_{2.72}/W_{18}O_{49}$ or WO_2, since both the amount of these phases increased in the seventh decomposition step.

But in the eight decomposition step, where practically only WO_2 formed, there was no heat change, so the heat effect between 700–750°C could not belong to the formation of WO_2. Thus, we explain the exothermic heat effect between 700–750°C as the formation and crystallization heat of γ-tungsten oxide, $WO_{2.72}/W_{18}O_{49}$. This phase is well defined and stoichiometric according to Booth *et al.* [31], which is shown also by the presence of sharp reflections in the XRD pattern at 750°C (Fig. 4). In fact, it is expected that an exothermic heat effect should accompany the transformation of the previous, not well defined $WO_{2.9}/W_{20}O_{58}$ (as well as $(NH_4)_{0.06}WO_3(H_2O)_{0.11}$) structure into the ordered $WO_{2.72}/W_{18}O_{49}$ phase, which corresponds to what we observed.

We are aware that traces of $WO_{2.72}/W_{18}O_{49}$ might have been already present in the sample at 670°C. We think that this small amount of $WO_{2.72}/W_{18}O_{49}$ might have formed, when the sample rearranged and ordered during cooling from 670°C. This might be the reason why the appearance of this small amount of $WO_{2.72}/W_{18}O_{49}$ did not cause an exothermic heat effect on the DTA curve up to 670°C.

Conclusions

Supplementing our earlier studies [16, 17], we investigated the reduction of APT directly up to 900°C by evolved gas analytical (TG/DTA-MS) and solid state (XRD and FTIR) measurements.

The formation of hexagonal ammonium and tetragonal hydrogen tungsten bronzes between 300–450°C seems to be two overlapping reactions, according to the themoanalytical curves. From tungsten bronzes, formation of reduced tungsten oxides ($WO_{2.9}/W_{20}O_{58}$, $WO_{2.72}/W_{18}O_{49}$, WO_2), and to a small degree that of tungsten metal were observed between 450–900°C, parallel to the stepwise formation of water, ammonia and nitrogen.

A previously unexplained exothermic DTA peak was detected between 700–750°C. We explained it as the formation and crystallization heat of γ-tungsten-oxide ($WO_{2.72}/W_{18}O_{49}$) from β-tungsten-oxide ($WO_{2.9}/W_{20}O_{58}$) and residual ammonium tungsten bronze.

Acknowledgements

One of the authors (I. M. S.) thanks for an Aschner scholarship of GE Hungary ZRt., GE Consumer & Industrial - Lighting.

References

1 E. Lassner and W.-D. Schubert, Tungsten. Properties, Chemistry, Technology of the Element, Alloys, and Chemical Compounds, Kluwer Academic/Plenum Publishers, New York 1999.
2 Special Issue on the Chemistry of Non-Sag Tungsten, (L. Bartha, E. Lassner, W.-D. Schubert and B. Lux, Eds), Int. J. Refract. Met. Hard Mater., 13 (1995) 1.
3 E. Pink and L. Bartha, The Metallurgy of Doped/Non-Sag Tunsgten, Elsevier, London 1989.
4 H.-J. Lunk, B. Ziemer, M. Salmen and D. Heidemann, Int. J. Refract. Met. Hard Mater., 12 (1993–1994) 17.
5 H.-J. Lunk, M. Salmen and D. Heidemann, Int. J. Refract. Met. Hard Mater., 16 (1998) 23.
6 A. Lackner, T. Molinari and P. Paschen, Scand. J. Metall., 25 (1996) 115.
7 J. W. van Put and T. W. Zegers, Int. J. Refract. Met. Hard Mater., 10 (1991) 115.
8 J. W. van Put and T. W. Zegers, Int. J. Refract. Met. Hard Mater., 13 (1995) 61.
9 Z. Zhang and M. Muhammed, Thermochim. Acta, 400 (2003) 235.
10 A. Biedunkiewicz, A. Szymczyk and J. Chrosciechowska, J. Therm. Anal. Cal., 77 (2004) 75.
11 S. Kano and T. Inouse, Surf. Coat. Technol., 201 (2006) 223.
12 H.-C. Kim, I.-J. Shon, J.-K. Yoon and J.-M. Doh, Int. J. Refract. Met. Hard Mater., 25 (2007) 46.
13 C. Moreno Castilla, M. A. Alvarez-Merino, F. Carrasco-Marín and J. L. G. Fierro, Langmuir, 17 (2001) 1752.
14 A. Szymańska-Kolasa, M. Lewandowski, C. Sayag and G. Djéga-Mariadassou, Catal. Today, 119 (2007) 7.
15 J. Madarász, I. M. Szilágyi, F. Hange and G. Pokol, J. Anal. Appl. Pyrol., 72 (2004) 197.
16 I. M. Szilágyi, J. Madarász, F. Hange and G. Pokol, Solid State Ionics, 172 (2004) 583.
17 I. M. Szilágyi, F. Hange, J. Madarász and G. Pokol, Eur. J. Inorg. Chem., 17 (2006) 3413.
18 J. Neugebauer, A. J. Hegedûs and T. Millner, Z. Anorg. Allg. Chem., 302 (1959) 50.
19 A. B. Kiss, Magy. Kém. Foly. (Hung.), 78 (1972) 302.
20 J. G. Lake and W. R. Ott, Thermochim. Acta, 32 (1989) 225.
21 N. E. Fouad, A. K. H. Nohman and M. I. Zaki, Thermochim. Acta, 239 (1994) 137.
22 N. E. Fouad, A. K. H. Nohman and M. I. Zaki, Thermochim. Acta, 343 (2000) 139.
23 O. Kirilenko, F. Girgsdies, R. E. Jentoft and T. Ressler, Eur. J. Inorg. Chem., 11 (2005) 2124.
24 M. Mészáros, J. Neugebauer and F. Hange, High Temp. Mater. Proc., 15 (1996) 111.
25 G. Gerey and G. Szigeti, MFKI Évkönyv (Hung.), (1977) 57.
26 L. Bartha and J. Neugebauer, Int. J. Refract. Met. Hard Mater., 13 (1995) 1.
27 G. K. Schwenke, M. Feist and H.-J. Lunk, J. Therm. Anal. Cal., 73 (2003) 3.
28 A. M. Garrido Pedrosa, M. J. B. Souza, D. M. A. Melo and A. S.Araujo, J. Therm. Anal. Cal., 87 (2007) 349.
29 NIST Chemistry Webbook Standard Reference Database, No. 69, 2005, June Release, http://webbook.nist.gov/chemistry
30 A. B. Kiss, T. Nemeth and E. Szalanczy, J. Mater. Sci., 13 (1978) 2541.
31 P. G. Dickens, A. C. Halliwell, D. J. Murphy and M. S. Wittingham, Trans. Farad. Soc., 67 (1971) 794.
32 J. Booth, T. Ekström, E. Iguchi and R. J. D. Tilley, J. Solid State Chem., 41 (1982) 293.
33 P. G. Dickens and M. S. Wittingham, Quart. Rev., 22 (1968) 30.
34 Gmelins Handbuch der Anorganischen Chemie, Achte Auflage, Stickstoff, System Nummer 4., Verlag Chemie, Berlin 1936.

DOI: 10.1007/s10973-006-8078-0